The Limit of Joint Penetration in High Energy Density Beam Welding

A theoretical means for predicting a limit to joint penetration is investigated

BY S. CHIANG AND C. E. ALBRIGHT

ABSTRACT. A theoretical limit of penetration for laser beam welding (LBW) is established to determine if further gains in joint penetration depth over existing process capability are theoretically possible. The penetration limit is calculated based on an analysis proposed by Swift-Hook and Gick with the assumption that the minimum bead width possible is equal to the diffraction limited focused spot size.

The current joint penetration capability of LBW is about 20% of the theoretical penetration limit when slow flowing helium is used as shielding gas. Penetration is improved to about 40% of the limit when plume suppression conditions are used, and about 50% in vacuum environments.

Hard vacuum electron beam welding achieves about 60% of the theoretical penetration limit, while nonvacuum electron beam welding ranges from 20% at low travel speeds to 60% at high travel speeds.

Introduction

Laser beam welding (LBW) and electron beam welding (EBW) are classified as high energy density welding processes. One of the characteristics of these two processes is the high aspect ratio (joint penetration depth to the weld width) of the weld metal compared to conventional arc welding processes. It is well known that the joint penetration depth of LBW is lower than that of electron beam welding at the same power level. The lower penetration in LBW is believed to be due to the formation of a laser-induced plume during welding (Refs. 1–3). This plume causes severe attenuation of the incident laser power. In recent years, various deep penetration techniques for laser beam welding have been developed through the control of the laser-induced plume (Refs. 2, 4, 5).

The maximum possible penetration depth or penetration limit of the laser beam welding process has, however, never been estimated. It is important to establish this limit to determine if any further gains in penetration over existing process capability are theoretically possible.

This paper is an attempt to establish a joint penetration limit based on the ability of a material to conduct heat away from the molten pool. In the case where heat is removed from the molten pool by conduction as fast as it can be supplied to the pool by the power beam, no further melting or penetration can occur. If the attenuation barrier and other barriers to joint penetration were completely removed, penetration would still be limited by this heat flow process.

S. CHIANG is with Rofin Sinar, Inc.; E. ALBRIGHT is with Department of Welding Engineering, The Ohio State University, Columbus, Ohio.

KEY WORDS

High Energy Welding
Laser Beam Welding
Laser Shielding Gases
Swift-Hook/Glick
Plume Suppression
Electron Beam Welding
Nonvacuum EB Welding
Hard Vacuum EB Welding
Penetration Limit
Beam Attenuation

Basis of Analysis

The volume of metal melted per unit time (V_M) in LB welding is dependent on a variety of process variables including laser power, power density, material properties, welding speed and focusing conditions. The analytical relationship between V_M and the power input, penetration depth and fusion zone width has been established by Hablanian and modified by Swift-Hook and Gick (Refs. 6, 7). By considering the heat conduction in a deep penetration welding process (Fig. 1), Swift-Hook and Gick developed an analytical solution as follows:

$$Y = 4\,Ur\,\{1-K_0^2(Ur)/K_1^2(Ur)\}^{1/2} \quad (1)$$

$$X = 2\,\pi\,\exp\{UrK_0\,(Ur)/K_1\,(Ur)\}/K_0(Ur) \quad (2)$$

where Y = dimensionless travel speed; X = dimensionless input power; K_0 = modified Bessel function of the 0 order; K_1 = modified Bessel function of the 1st order

The term "Ur," defined as the product of the travel speed divided by the thermal diffusivity times the radius of the melting point isotherm, was introduced as a dummy variable. In this study, a range of Ur values covering all characteristic values was introduced for calculations of X and Y. For each value of Ur produced, a corresponding set of values for a welding travel speed, v, and penetration, a, were calculated by:

$$v = YD/b \quad (3)$$

$$a = W/XS \quad (4)$$

Where S = k (Tm – To), the heat function; k = average thermal conductivity;

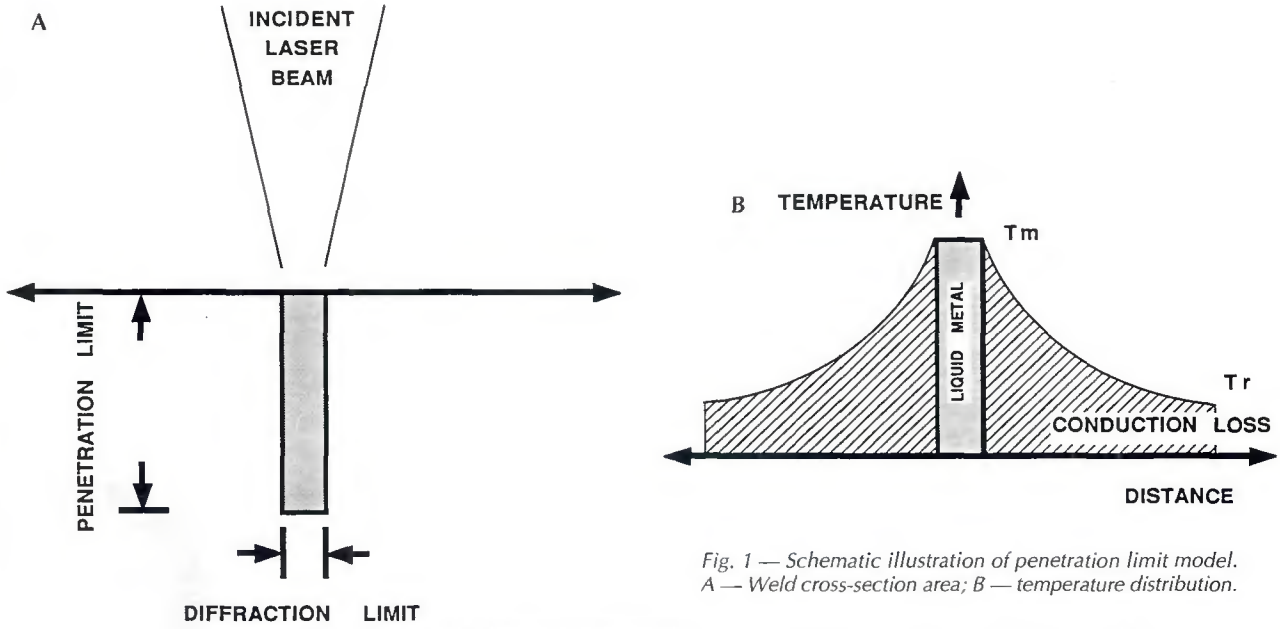

Fig. 1 — Schematic illustration of penetration limit model. A — Weld cross-section area; B — temperature distribution.

Tm = melting temperature; To = ambient temperature; and W = input power to the weld.

The weld width, b, was taken to be the minimum value possible to maximize penetration and establish a theoretical penetration limit. This value was taken to be the diffraction limited focused spot diameter for laser welds, and the reported focused spot diameter for electron beam welds.

In calculating the penetration limit for the LBW process, all the laser power absorbed by the workpiece is removed by thermal conduction into the base metal. Other types of power loss through reflection, radiation, convection, or beam attenuation are not considered for this ideal maximum penetration condition. Additional necessary assumptions include:

1) The weld has a constant width — Fig. 1.

2) Fluid flow is neglected (as in the Swift-Hook and Gick model).

Swift-Hook and Gick classified the heat flow characteristics of both LBW and EBW into two dimensionless regions, *i.e.*, a low travel speed region and a high travel speed region. In the low-speed region, the conduction loss through the unmelted base metal is very large and the melting efficiency falls dramatically with decreasing travel speed. The relationship between penetration depth and the process variables in this region can be expressed as:

$$(vb/D) = \exp\,[1.502 - 6.28\,(aS/W)] \qquad (5)$$

In the high-speed region, the melting efficiency is improved to a limit of 48% according to Swift-Hook and Gick. The relationship of two dimensionless factors is linear:

$$(vb/D) = 0.483\,(W/aS) \qquad (6)$$

Note that from Equations 5 and 6 the range of either the low- or high-speed regions is determined by the thermal properties of the base metal and the efficiency of power transfer, as well as the travel speed. If the input power, material, and welding speed are given, the penetration depth is not known until the bead width is measured through experiment. Swift-Hook and Gick's analysis cannot be applied to directly predict joint penetration depth without assuming a weld bead width.

The penetration capability of laser beam welding is also a function of the laser light source and the beam delivery system. The laser beam transverse electromagnetic mode (TEM), beam size and the focusing conditions have strong influences on the penetration depth of laser beam welding (Ref. 8). Relationships are available to calculate the dimensions of a focused beam if the TEM conditions are known (Ref. 8). Sasnett (Ref. 9) proposed a beam mode factor, M^2, to determine the deviation of a higher order mode laser beam from a Gaussian (TEM_{00}) mode beam. For a TEM_{00}, M^2 has the lowest possible value of 1. This factor can be used directly to simplify optical calculations by comparing any given beam to the ideal Gaussian beam. The diffraction limited minimum focused spot size, D_0, can be obtained from the following equation (Ref. 9):

$$D_0 = 4\,M^2\,L\,f/\pi\,d \qquad (7)$$

where d = beam diameter at focusing lens; f = focal length of the lens; M^2 = beam mode factor, 1 for Gaussian mode; L = wavelength, 10.6 μm for CO_2 laser.

The focused spot size can be reduced by decreasing M^2 (by approaching a Gaussian beam condition). Reducing the focal spot size increases the power density (power/unit area) and increases joint penetration (Ref. 5).

A calculation of the penetration limit for LBW can be made based on the Swift-Hook and Gick model if the assumption is made that the smallest possible bead width is the minimum diameter of the focused beam. It is noted that the minimum bead width will produce the maximum penetration in this mode.

The results of a calculation of the penetration limit for a 2-kW Gaussian laser beam focused with a 12.7-cm focal length lens are illustrated in Fig. 2. Referring to Fig. 2, the low-speed limit function forms the thin line at low speeds, and the high-speed limit function (*i.e.* 48% melting efficiency) forms the thin line at high speeds. The thick line that diverges from the low-speed function and joins with the high-speed function with increasing travel speed is the curve formed by the complete theoretical model. Note that the penetration limit curve in Fig. 2 is only applicable to laser welds on steel made with a 2-kW Gaussian beam (M^2 = 1) at focus using a 12.7-cm focal length lens. Variation in power level affects both the low-speed and high-speed regions.

This analysis is not appropriate at either very slow travel or very rapid travel speeds. At very slow travel speeds, the molten pool is very large and the penetration cavity is unstable. At very rapid travel speeds, the penetration cavity be-

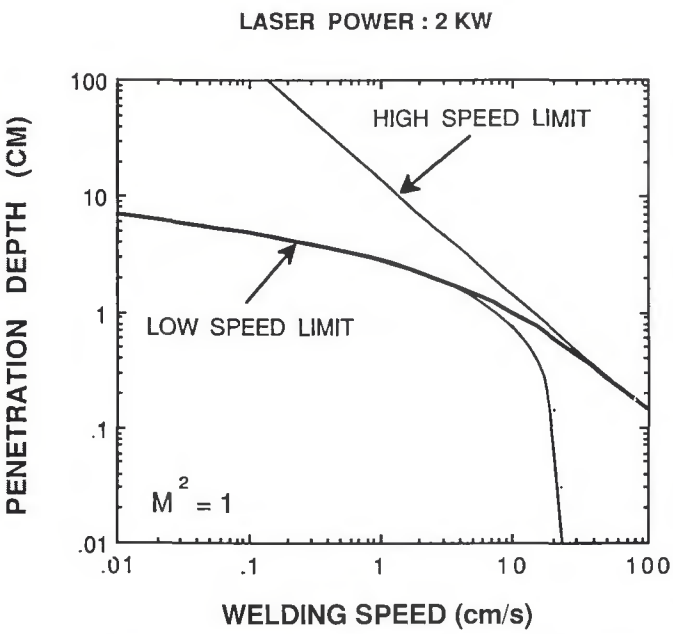

Fig. 2 — Penetration depth limit curve for a Gaussian laser beam at 2-kW power.

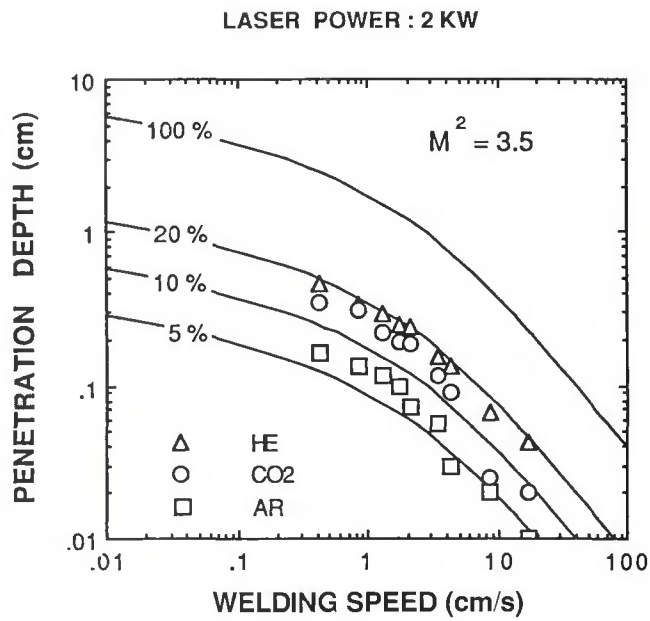

Fig. 3 — Effects of shielding gases on penetration depth for a 2-kW laser beam, M2 value of 3.5.

comes diminishingly small.

Discussion

Penetration Limit and Current Penetration Status

Penetration in LBW is hindered at both very low speeds and very high speeds. At extremely low welding speeds, the stability of the vapor cavity will determine the penetration depth for both LB and EB welding (Refs. 2, 10). The collapse of liquid metal in the side walls of the vapor cavity will seal the vapor cavity and block the incident beam, preventing further penetration.

The vapor cavity will gradually disappear due to the decreased power per unit length of weld at very high welding speeds. In the resulting shallow penetration condition, the three-dimensional heat transfer conditions apply for both the LB and EB welding processes. Thus, two-dimensional thermal analysis is no longer valid. The vapor cavity tends to trap light, which increases beam power input efficiency. As the vapor cavity disappears with increasing travel speed, the power input efficiency is reduced due to decreased light trapping. The effects combine to further reduce penetration in the high-speed region.

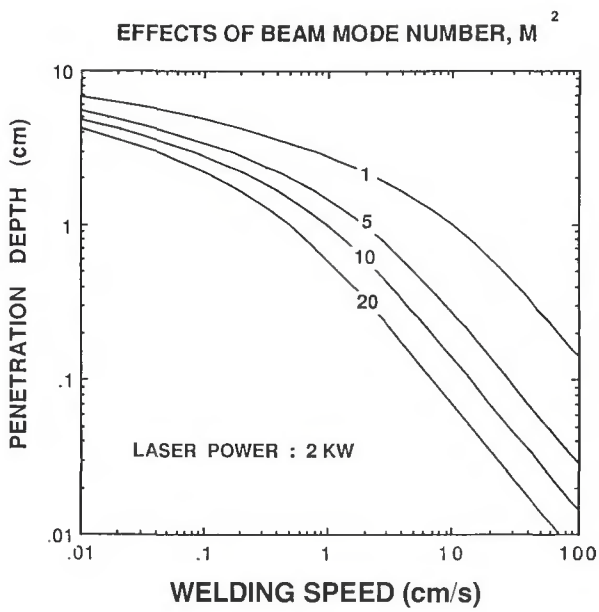

Fig. 4 — Effects of laser beam mode on joint penetration depth limit.

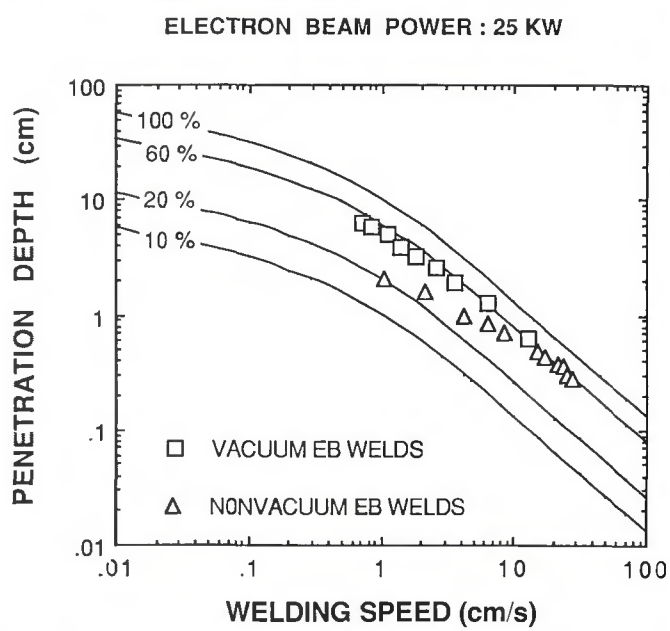

Fig. 5 — Joint penetration capabilities of vacuum and nonvacuum electron beam welding processes.

Table 1 — LBW Parameters

Laser system	Coherent General M53 3-kW CO_2 laser
Lens	ZnSe, 12.7 cm focal length
Beam size	1.8 cm at lens surface
Focus location	on specimen surface
Beam mode	near Gaussian mode, $M^2 = 3.5$
Diffraction limit	0.00952 cm in diameter
Shielding gas	He, CO_2, Ar
Power level	2 kW on power meter
Material	1018 carbon steel
Weld style	bead on plate

Comparison of Theory and Experiment

In Fig. 3, the penetration limit is compared with the measured penetration depth for LB welds at 2 kW CO_2 laser power on AISI 1018 carbon steel. A 12.7-cm zinc selenide lens was used for focusing. The M^2 value of the beam was estimated to be 3.5 based on beam mode measurements made at Coherent General Corp. Each penetration data point is averaged from at least three tests. Tests were performed in slow flowing shielding gas without any plume-suppression nozzle. Details of the welding conditions are listed in Table 1. The lines indicated as 5, 10 and 20% on Figs. 3, 4 and 10, 20 and 60% on Fig. 5, represent the percent of maximum theoretical penetration calculated by this model.

The penetration depth data for helium shielded LB welds are grouped about a curve at 20% of the calculated penetration limit. Welds made in helium under similar conditions but at 1.5 and 2.5 kW also yielded penetrations of 20% of the calculated penetration limit at the respective power levels. These observed penetration values are quite comparable to other published penetration values (Ref. 11).

A number of investigators have developed deep penetration techniques for LBW in the past few years (Refs. 2, 4, 5). These penetration data cannot be directly applied to the calculated penetration limit due to lack of experiment details. However, the enhanced penetration is generally about twice the penetration obtained using slow flow shielding gas. Thus, the penetration capability is improved to about 40% of the penetration limit using these plume suppression techniques, and slightly higher (about 50%) for vacuum environment LBW.

The penetration in LBW is low compared to either the proposed penetration limit or the penetration depth of EB welding (shown to be 60% or more of the calculated penetration limit later in this discussion). Thus, there is significant potential for improved penetration in the LBW process.

Effects of Shielding Gas

It is known that the type of shielding gas will affect the penetration depth of laser beam welding (Refs. 1–5, 12–15). In this investigation, helium shielded welds gave the best penetration results while argon shielded welds yielded very poor penetration (4 to 8% of the penetration limit — Fig. 3). The mechanisms causing differences in penetration depth for various shielding gases are still being debated (Refs. 1–5, 14, 15). However, this phenomenon can be viewed in terms of attenuation effects of incident laser beam.

Another important conclusion drawn from Fig. 3 is that the attenuation factor is a constant for a given shielding gas in the tested welding speed range. In Equation 1, one may notice that for a given welding speed and bead width, the ratio between power level and the penetration remains constant. The observation that the fraction of ideal penetration remains constant with variation in travel speed indicates that there is a constant fraction of beam power being blocked from entry to the weld pool. The value of attenuation factor for each type of shielding gas is being investigated. However, the relative attenuation effects are clearly shown in Fig. 3. The shallow penetration in an argon atmosphere is thus the result of severe beam attenuation. The attenuation effect is not as severe when helium or CO_2 gas is used.

This apparent constant attenuation effect seemed to hold for the laser welding conditions presented in this investigation, but care must be taken in considering this effect to be "universal." At higher power levels, complete attenuation can occur in large argon plumes.

Effects of Beam Mode

The laser beam mode is another factor affecting the penetration limit for a given power. As presented in Fig. 4, the penetration limit curve will shift down for higher laser beam TEM numbers (when M^2 increases). This decrease in penetration limit is the result of increasing diffraction limited focused spot size, and thus, a wider minimum bead width. The loss of penetration capability is clearly a disadvantage for a high TEM number laser beam.

As predicted by the theory (Fig. 4), the high-speed region is obtained at lower welding travel speeds when using a high TEM mode beam (large M^2 number). This is mainly due to the conduction losses, which increase for high TEM mode laser beams at low travel speeds.

Vacuum and Nonvacuum EB Welding

The calculation of the penetration limit for EB welding at 25 kW was performed in a similar way as the calculation for LB welding. The only difference in the calculation is that the minimum weld bead width (or focused spot size) is taken from empirically measured spot size data. For a 25-kW electron beam, the spot size was assumed to be 0.127 cm (0.05 in.) in diameter (Ref. 16). The penetration data of EB welding was converted from the *Welding Handbook* data (Ref. 17).

As shown in Fig. 5, hard vacuum EB welding penetration depth data are located along a line representing 60% of the penetration limit. Compared to LB welding data (20% in He, about 40% with plume suppression jets, and about 50% in vacuum), electron beams have a clear edge in approaching the theoretical penetration limit.

For nonvacuum EB welding, the penetration depth is reduced from 60 to 20% as the travel speed is reduced from the high-speed to the low-speed region — Fig. 5. This implies that there is an attenuation phenomenon similar in magnitude to the attenuation observed in LBW in helium.

Conclusions

The following conclusions can be drawn from this investigation:

1) A theoretical limit of joint penetration for laser beam welding can be calculated based on an analysis proposed by Swift-Hook and Gick if the assumption is made that the minimum bead width possible is equal to the diffraction limited focused spot size.

2) The penetration capability of the LBW experiments presented here (1.7 kW, $M^2 = 3.5$, 5-in. focal length lens, slow flowing helium shielding) are about 20% of the theoretical limit developed using the Swift-Hook and Gick analysis. This fraction of the penetration limit was relatively constant over a broad range of travel speeds, suggesting a constant factor of beam attenuation.

Acknowledgment

The authors wish to thank the Edison Welding Institute for financial support for this work.

References

1. Herziger, G. 1986. The influence of laser-induced plasma on laser material processing. *The Industrial Laser Annual Handbook*, D. Belforte and M. Levitt, eds., pp.108–115. Tulsa, Pennwell.

2. Banas, C. M. 1986. High power laser welding. *The Industrial Laser Annual Handbook*, D. Belforte and M. Levitt, eds., pp. 69–86. Tulsa, Pennwell.

3. Matsunawa, A., Yoshida, H., and Katayama, S. 1984. Beam-plume interaction in pulsed YAG laser processing.*ICALEO '84* Vol. 44, J. Mazumder, ed., pp. 35–42, Laser Institute of America, Toledo, Ohio.

4. Brown, C. O., and Banas, C. M. 1986. High-power laser beam welding in reduced-pressure atmospheres. *Welding Journal* 65(7):48–52.

5. Arata, Y. 1986. The role of assist gas in CO_2 laser welding. *Plasma, Electron & Laser Beam Technology*, Y. Arata, ed., pp. 498–505. ASM International, Materials Park, Ohio.

6. Hablanian, M. H. 1963. A correlation of welding variables. *Proc. of the 5th Symposium on Electron Beam Technology*, J. R. Moreley, ed., pp. 262–268, Alloyd Electronics, Cambridge, Mass.

7. Swift-Hook, D. T., and Gick, A. E. F. 1973. Penetration welding with lasers. *Welding Journal* 52(11):492-s to 499-s.

8. Luxon, J. T. 1986. Optics for materials processing. *The Industrial Laser Annual Handbook*, D. Belforte and M. Levitt, eds., pp. 38–48, Tulsa, Pennwell.

9. Sasnett, M. W. 1985. Propagation of multimode laser beams — the M^2 factor. *CLEO '85*, American Society of Optics, Washington D.C.

10. Schauer, D. A., and Giedt, W. H. 1978. Prediction of electron beam welding spiking tendency. *Welding Journal* 57(7):189-s to 195-s.

11. Laser material processing data guidelines. 1986. *The Industrial Laser Annual Handbook*, D. Belforte and M. Levitt, eds., p. 4, Tulsa, Pennwell.

12. Arnot, R. S., and Albright, C. E. 1983. Plasma plume effects in pulsed carbon dioxide laser spot welding. *ICALEO '83* Vol. 38, E. A. Metzbower, ed., 51–58, Laser Institute of America, Toledo, Ohio.

13. Chennat, C., and Albright, C. E. 1984. Shielding gas effects in pulsed carbon dioxide laser spot welding. *ICALEO '84* Vol. 44, J. Mazumder, ed., pp. 76–85, Laser Institute of America, Toledo, Ohio.

14. Chiang, S. and Albright, C. E. 1988. A review of light/material interactions during laser material processing. EWI Research Report Vol. MR8817, Edison Welding Institute, Columbus, Ohio.

15. Dausinger, F., Beck, M., Rudlaff, T., and Wahl, T. 1988. On coupling mechanisms in laser processes. *Laser in Manufacturing* Vol. 5:177–185, H. Hugel, ed., ISF Ltd., Kempston, Bedford, U. K.

16. Prof. W. H. Giedt, April 1989.

17. Data taken from *Welding Handbook*, Vol. 3, 7th ed. Chap. 5. Electron beam welding. pp. 175 and 200, American Welding Society, Miami, Fla.